Current Biology *16*, 433–439, February 21, 2006 ©2006 Elsevier Ltd All rights reserved DOI 10.1016/j.cub.2006.01.018

Report

The Human RNA Surveillance Factor UPF1 Is Required for S Phase Progression and Genome Stability

Claus M. Azzalin[1,2] and Joachim Lingner[1,2,*]
[1] Swiss Institute for Experimental Cancer Research (ISREC)
Ecole Polytechnique Fédérale de Lausanne (EPFL)
[2] NCCR Program Frontiers in Genetics
155 Chemin des Boveresses
CH-1066 Epalinges s/Lausanne
Switzerland

Summary

The eukaryotic *n*onsense-*m*ediated mRNA *d*ecay (NMD) pathway degrades mRNAs carrying premature stop codons (PTC). In humans, NMD depends on the RNA- and DNA-dependent 5′-3′ helicase UPF1 and six other gene products referred to as SMG1, UPF2, UPF3, EST1A/SMG6, EST1B/SMG5, and EST1C/SMG7. The NMD machinery is also thought to coordinate mRNA nuclear export and translation and to regulate the levels of several physiologic transcripts [1–7]. Furthermore, in a process named SMD, UPF1 promotes degradation of mRNAs that are bound by Staufen 1 [8]. Intriguingly, SMG1 and EST1A/SMG6 function also in DNA repair and telomere maintenance, respectively [9–11]. Here, we show that UPF1 is also required for genome stability. shRNA-mediated depletion of UPF1 causes human cells to arrest early in S phase, inducing an ATR-dependent DNA-damage response. A fraction of hyperphosphorylated UPF1 associates with chromatin of unperturbed cells, and chromatin association increases in S phase and upon γ irradiation. ATR phosphorylates UPF1 both in vitro and in vivo, and shRNA-mediated downregulation of ATR diminished the association of UPF1 with chromatin, although it did not affect NMD. Physical interaction of UPF1 with DNA polymerase δ suggests a role for human UPF1 in DNA synthesis during replication or repair.

Results and Discussion

To study the physiological role of human UPF1, we transfected HeLa cells with two shRNA vectors (shRNAI and shRNAII) targeting different 19 nucleotide regions of the UPF1 mRNA. Western-blot analysis shows that both shRNAs efficiently reduce UPF1 levels to 10%–20% 5 days after transfection (Figure 1A). As expected, shRNAI- and shRNAII-mediated depletion of UPF1 leads to stabilization of the PTC-containing reporter mRNA β-globin^{NS39} (Figure S1 in the Supplemental Data available online) and of an endogenous PTC-containing ABCC4 splice variant (ABCC4^{SV2}, see below) known to be constantly degraded by NMD [12]. Four to seven days after transfection with shRNAI and shRNAII, HeLa cells stopped proliferating and showed severe morphological changes, with cytoplasm and nuclei enlarging 3–5-fold (Figure S2). The capacity to form colonies was reduced 20–50-fold (Figure 1B). This was not attributable to apoptosis because cells did not stain positive for the apoptotic marker Annexin V, nor did they exhibit Caspase activation (data not shown). Similar results were obtained with the renal epithelial cell line 293T, the fibrosarcoma-derived cell line HT1080, and the osteosarcoma-derived U2OS cells (data not shown).

As determined by flow cytometry, cells depleted for UPF1 accumulate with a DNA content slightly higher than 2*n* (M1 region in Figure S2), potentially corresponding to early S phase. Consistently, a 1:1 mixture of cells transfected with empty vector and with shRNAII produced a peak in between the G1 peak of the empty vector and the M1 peak of the UPF1-shRNA-treated cells (Figure S2). UPF1 depletion also induces the appearance of cells with DNA content higher than *4n*. The >4*n* cells may correspond to the cells with enlarged nuclei observed by microscopic inspection (Figure S2). Normal cell-cycle distribution was restored when shRNAII vector was cotransfected with a plasmid driving the expression of a transgenic Flag-UPF1 protein (F-UPF1^{2054}) from a cDNA with the shRNAII target site mutated (Figure S3). This confirms that the described cell-cycle defect was due to depletion of UPF1 and was not caused by off-target effects. Importantly, cells shRNA-depleted for the NMD factor UPF2 [13] progressed normally through the cell cycle (Figure S2), whereas NMD was impaired (Figure S1). This suggests that the defective cell-cycle progression of UPF1-depleted cells is not due to loss of general NMD.

To verify the early S phase arrest in UPF1-depleted cells, we measured DNA synthesis by pulse labeling with bromodeoxyuridine (BrdU) for 15 hr between days 3 and 4 after transfection. In the empty-vector sample, a large fraction (80%) of the cells was BrdU positive and distributed in all phases of the cell cycle (Figure 1C). In the shRNA samples, a lower number of cells was BrdU positive (14% for shRNAI and 55% for shRNAII), confirming that UPF1 depletion perturbs cell-cycle progression. Furthermore, a large fraction (71%) of BrdU-positive cells had a similar DNA content (referred to as R1 in Figure 1C). We also used an anti-PCNA monoclonal antibody to stain shRNA-treated cells after methanol fixation in order to specifically detect PCNA associated with replication forks [14, 15]. The fraction of PCNA-positive cells increased upon UPF1 depletion, and the intranuclear distribution pattern of PCNA foci indicated that the vast majority of these cells were in early S phase (Figure 1D). We conclude that UPF1-depleted cells can initiate but not complete DNA replication.

Inhibition of DNA replication-fork progression triggers a DNA-damage response [16–18]. Therefore, we stained UPF1-depleted cells with antibodies against phosphorylated histone H2AX (γ-H2AX), a sensitive marker for damaged DNA. The fraction of γ-H2AX-positive cells increased significantly in UPF1-shRNA-treated cells from

*Correspondence: joachim.lingner@isrec.ch

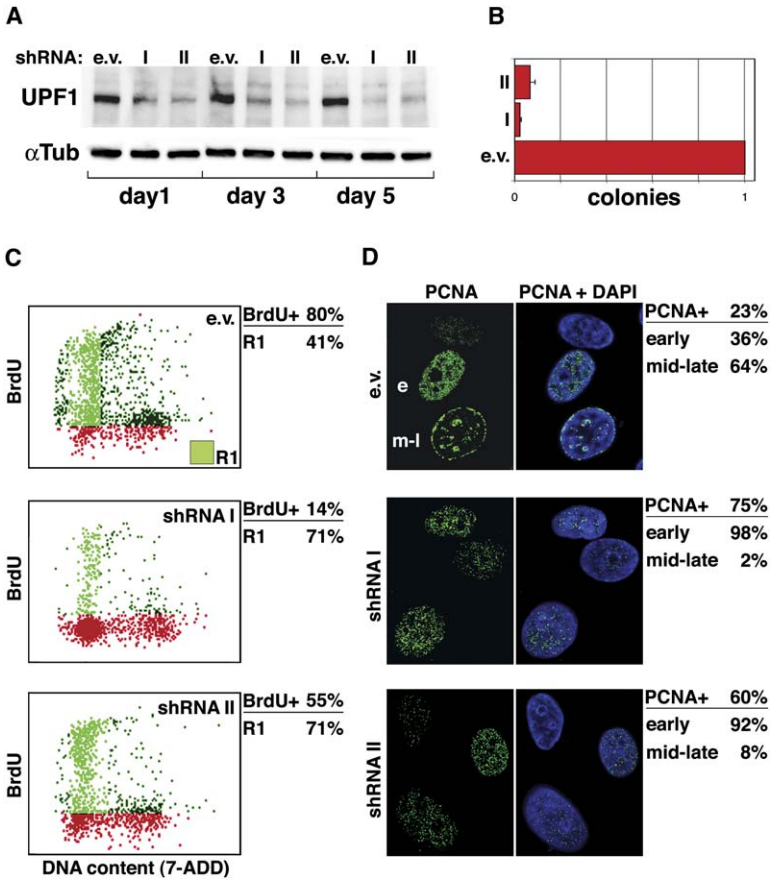

Figure 1. shRNA Depletion of UPF1 Induces S Phase Arrest in HeLa Cells

(A) HeLa cells were transfected with empty-vector control (e.v.) and with anti-UPF1 shRNA vectors I and II. After 1, 3, and 5 days, total protein was extracted, and expression of UPF1 was assessed by western blotting. α-Tubulin was used as loading control.

(B) Colony-forming assay of HeLa cells depleted for UPF1. Cloning efficiency of the shRNA-treated cells is expressed relative to the empty-vector control from three independent experiments.

(C) BrdU incorporation in HeLa cells transfected with shRNAI and shRNAII and with empty-vector control. Pulse labeling was performed for 15 hr between days 3 and 4 after transfection. BrdU incorporation (*y* axis) was determined by using FITC-labeled anti-BrdU antibody, and DNA content was measured with 7-aminoactinomycin D (7-ADD; *x* axis). BrdU-negative cells are shown in red, and BrdU-positive cells are shown in green. Percentages indicate the total fraction of BrdU-positive cells (BrdU+) and the fraction of BrdU positive cells that accumulate in the R1 region (light green).

(D) PCNA staining of HeLa cells fixed with methanol 4 days after transfection with shRNAI and shRNAII and with empty-vector control. The PCNA signal is shown in green; DAPI-stained DNA is shown in blue. The total fraction of PCNA-positive cells and the fraction of PCNA positive cells showing a PCNA pattern characteristic of early (e) and middle-late (m-l) S phase are indicated. One hundred cells were scored for each sample. The results presented in (C) and (D) are from independent representative experiments.

approximately 22% to 58% (Figures 2A and 2B). Furthermore, the overall intensity of the individual γ-H2AX foci observed in empty-vector-transfected cells was considerably lower than that observed in shRNA-treated cells. Expression of shRNA-resistant F-UPF1^{2054} rescued the cells from accumulating γ-H2AX (Figure S3), proving that the DNA-damage response was an authentic outcome of UPF1 depletion. As for the cell-cycle defect, γ-H2AX accumulation was not observed in U2OS cells depleted for UPF2 (Figure 2B), supporting an NMD-independent role for UPF1 in S phase progression and genome stability. However, this does not rule out involvement of the UPF1-dependent (and UPF2-independent) SMD [8]. Consistent with the accumulation of DNA damage, metaphases that could be prepared from UPF1-depleted cells relieved from cell-cycle arrest upon treatment with the phosphoinositide-3-kinase-related kinase (PIKK) inhibitor caffeine showed a 3-fold increase in the total number of chromatid breaks and a 8–9-fold increase in the total number of chromosome breaks (Table 1 and Figure S4). Accumulation of acentric fragments, dicentrics, and radial chromosomes was also observed. These observations were further substantiated by using a single-cell gel-electrophoresis assay ("comet assay"), in which nuclei release broken DNA fragments upon migration in an electric field (Figure S4). We speculate that the observed chromosomal aberrations arose at the sites where the replication forks arrested because of UPF1 depletion.

Phosphorylation of H2AX is mediated by the PIKKs ATM and ATR, which become activated upon DNA damage [17, 18]. Immunostaining and western-blot analysis of shRNA-treated U2OS and HeLa cells with antibodies against activated ATM (phosphorylated at Ser 1981) showed no significant activation of this kinase (Figure 2C and data not shown). Consistently, western-blot experiments also failed to detect phosphorylation of the ATM substrate CHK2 (data not shown). To test for activation of ATR, we used U2OS-derived GW33 cells stably expressing FLAG-epitope-tagged ATR [19]. Flag-tagged ATR protein formed foci in more than 60% of the cells treated with shRNA against UPF1, whereas fewer than 10% of the empty-vector-treated cells showed ATR foci (Figure 2C). We then performed double-transfection experiments with shRNAs against UPF1 and ATM or ATR [20, 21] (validated in Figure S1). In cells depleted for both ATM and UPF1, γ-H2AX was induced to a similar extent as in cells depleted for UPF1 only. In contrast, when cells were simultaneously depleted for both ATR and UPF1, γ-H2AX levels were substantially reduced (Figure 2D). Thus the DNA-damage response induced by UPF1 depletion is largely mediated by ATR. This is consistent with the observation that UPF1-depleted cells arrest in S phase, because ATR is thought to be the PIKK primarily involved in regulating the cellular response to replication block [17, 18].

To test for a direct role of UPF1 in DNA metabolism, we prepared soluble and chromatin-associated protein

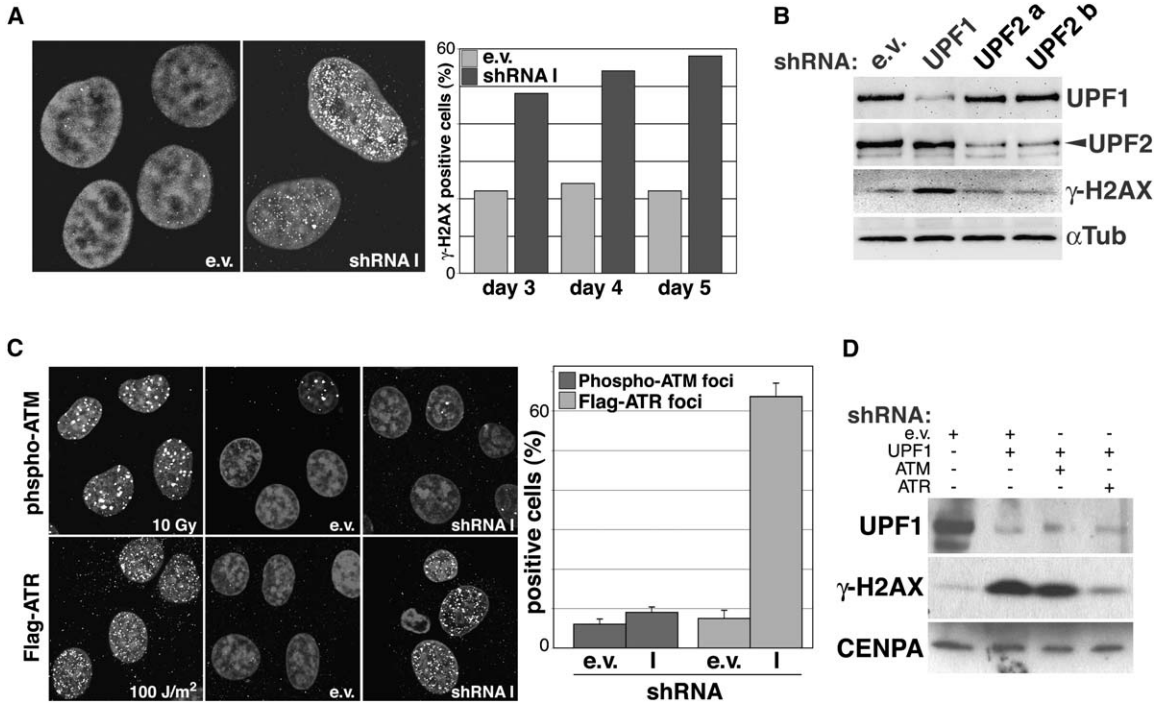

Figure 2. shRNA Depletion of UPF1 Induces an ATR-Dependent DNA-Damage Response

(A) HeLa cells were transfected with shRNAI and with empty-vector control and stained with mouse monoclonal antibodies against γ-H2AX (white signal). DAPI-stained DNA is shown in gray. The graph illustrates the fraction of cells with at least four γ-H2AX foci (positive cells) detected in empty-vector control and in shRNAI-treated cells 3, 4, and 5 days after transfection. Data are from one representative experiment where 50 cells were scored for each time point.

(B) U2OS cells were transfected with empty vectors, UPF1 shRNAI, and two independent shRNAs against UPF2. UPF1, UPF2, and γ-H2AX protein levels were assessed by western blotting 4 days after transfection. α-Tubulin was used as loading control.

(C) U2OS and GW33 cells were transfected with shRNAI and with empty-vector control. Three days after transfection, cells were stained with anti-phospho-ATM Ser1981 (U2OS cells) and with anti-Flag monoclonal antibodies (GW33). As positive controls, cells were γ-irradiated with 10 Gy or UV-irradiated with 100 J/m^2 and processed 2 hr after treatment. ATM and Flag-ATR foci are shown in white. The graph shows quantification of cells containing at least four phospho-ATM or 4 Flag-ATR foci (positive cells). Mean percentage values were obtained from two independent experiments and expressed as a fraction of the total number of cells (50) analyzed in each experiment. Error bars indicate the mean ± standard deviation for two experiments.

(D) HeLa cells were simultaneously transfected with shRNA against UPF1 (shRNAI) and ATM or ATR kinases. Four days after transfection, total-cell extracts were prepared and the levels of UPF1 and γ-H2AX were determined by western blotting. CENPA was used as loading control.

fractions from HeLa cells [22]. The majority of UPF1 protein was detected in the soluble fraction. Nevertheless, a significant fraction of UPF1 (about 4%) was chromatin bound (Figure 3A and Figure S5). Supporting these observations, chromatin-immunoprecipitation experiments of formaldehyde cross-linked cells, followed by detection of Alu-element-containing genomic DNA, showed association of UPF1 with about 2% of input DNA (Figure S5). Strikingly, a 4-fold increase of the amount of chromatin-associated UPF1 was detected in cells enriched in S phase upon the release from a hydroxyurea block (Figure S5). As expected, the nuclear marker nucleolin and the cytoplasmic marker α-tubulin were detected only in the soluble fraction. In contrast and consistent with published results [22], PCNA was present in the insoluble fractions from nonsynchronized cells, and its association strongly increased in S phase as observed for UPF1 (Figure 3 and Figure S5). It is possible that at least a part of the UPF1 association with chromatin upon hydroxyurea treatment is due to the DNA damage derived from nucleotide depletion. Therefore, we also released cells from a nocodazole-induced metaphase block and followed the kinetics of the UPF1 chromatin association (Figure 3A). Cell-cycle progression was tracked by FACS analysis (data not shown). Whereas minor fluctuations of UPF1 were observed in the soluble

Table 1. Chromosomal Aberrations in HeLa Cells Depleted for UPF1

	Analyzed Metaphases	# Chromosomes/ Metaphase	Chromatid Breaks (tot #)	Chromosome Breaks (tot #)	Dicentrics (tot #)	# Metaphases ≥ 5 Chromatid Breaks	# Metaphases ≥ 1 Chromosome Breaks
Empty vector	25	73.8 ± 5.4	79	2	3	6	2
shRNAI	24	69.3 ± 15.1	221	16	10	21	9
shRNAII	25	71.8 ± 7.6	233	18	9	19	12

Results are from one representative experiment.

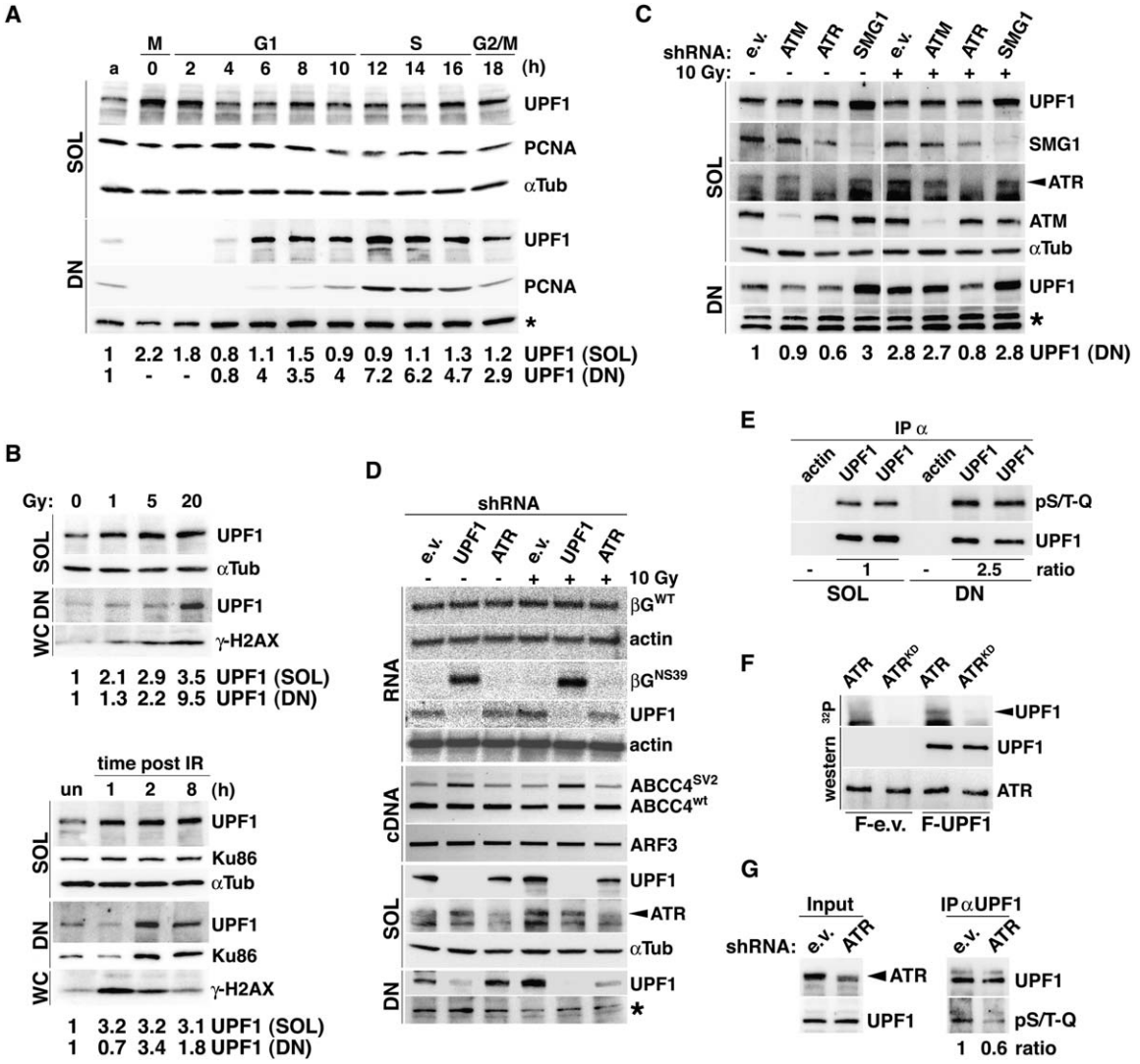

Figure 3. UPF1 Associates with the Chromatin of Untreated and γ-Irradiated HeLa Cells through ATR-Mediated Phosphorylation

(A) HeLa cells were blocked in mitosis with Nocodazole for 12 hr and then released from the block. Soluble (SOL) and DNA-bound (DN) protein extracts were prepared every 2 hr over a time course of 18 hr, and UPF1, PCNA, and α-Tubulin levels were assayed by western blotting. Numbers at the bottom indicates the levels of soluble and DNA-bound UPF1 expressed relative to UPF1 signal in the asynchronous sample (indicated by a) after normalization with the signal of α-Tubulin and an unspecific cross-reacting band (asterisk) detected with an unrelated rabbit serum. Different phases of the cell cycle are indicated.

([B], upper panels) HeLa cells were γ-irradiated with 0, 1, 5, and 20 Gy, and soluble and DNA-bound protein fractions as well as whole-cell extracts (WC) were prepared 2 hr after irradiation and assayed for UPF1, α-Tubulin, and γ-H2AX.

([B], lower panels) HeLa cells were γ-irradiated with 10 Gy, and soluble and DNA-bound protein fractions as well as total-cell extracts were prepared 1, 2, and 8 hr after irradiation and assayed for UPF1, Ku86, α-Tubulin, and γ-H2AX. Numbers at the bottom indicate the levels of soluble and DNA-bound UPF1, normalized for total protein content with the α-Tubulin signal and expressed relative to the UPF1 signal in the untreated (un) sample.

(C) HeLa cells were transfected with shRNA vectors against ATM, ATR, or SMG1 kinases. Four days after transfection, cells were irradiated with 0 or 10 Gy, and UPF1, SMG1, ATR, and ATM were detected by western blotting. The α-Tubulin signal and an unspecific band (asterisk) detected with an unrelated rabbit serum were used as normalization controls for protein loading in soluble and DNase fractions, respectively. Numbers are as in (B).

(D) HeLa β-globin^{WT} (two upper panels) and HeLa β-globin^{NS39} (other panels) cells were transfected with shRNAs against UPF1 (shRNAII) and ATR. Four days after transfection, cells were γ-irradiated with 0 and 10 Gy. Two hours later, total RNA, soluble proteins, and chromatin-bound proteins were prepared. Northern-blot analysis was performed to detect β-globin^{WT}, β-globin ^{NS39}, and UPF1 mRNAs; RT-PCR analysis was used to detect ABCC4 wild-type (wt) and splice variant 2 (SV2) containing a PTC; western-blot analysis was performed to detect UPF1 and ATR. Actin, ARF3, α-Tubulin, and an unspecific band (asterisk) from an unrelated rabbit serum were used as loading controls in the different experiments.

(E) Soluble and DNase fractions were prepared from HeLa cells, and endogenous UPF1 was immunoprecipitated by using goat polyclonal antibodies. Parallel IP experiments using goat polyclonal antibodies against actin were performed to control for IP specificity. Immunoprecipitated material was blotted to nitrocellulose membranes and probed with anti-phospho-S/T-Q and anti-UPF1 antibodies (UPF1 IP is shown in duplicate). Numbers indicate the mean ratio of anti-phospho-S/T-Q signal relative to the anti-UPF1 signal for the same sample. Values are normalized to the signal in the soluble samples.

(F) Immunopurified Flag-tagged ATR and ATR kinase dead (ATR^{KD}) were incubated with immunopurified Flag-tagged UPF1 (F-UPF1). Control experiments were performed with empty-vector control (F-e.v.). Kinase reactions were performed in presence of γ-[^{32}P]ATP. Proteins were

fraction, its chromatin association was strongly dependent on the cell-cycle stage. The levels of chromatin-bound UPF1 were very low in mitosis and early G1, started to increase in mid-G1, and reached highest values in S phase (about 6–7-fold increase compared to the asynchronous population). Upon S phase exit, chromatin association of UPF1 started again to diminish. In this experiment, chromatin association of PCNA showed similar cell-cycle dependence as UPF1.

We then set out to test whether UPF1 was responding to DNA damage. HeLa cells were γ-irradiated, and UPF1 association with chromatin was assayed 2 hr after irradiation. Soluble UPF1 levels increased 2–3.5-fold upon different doses of γ irradiation (Figure 3B), correlating with an approximately 2-fold increase of UPF1 mRNA (Figure 3D). Strikingly, a more pronounced γ-ray dose-dependent increase of UPF1 (up to 9.5-fold increase with 20 Gy) was observed in the chromatin-bound fractions (Figure 3B). Consistently, chromatin-immunoprecipitation experiments showed a 12-fold increase in the amount of DNA associated to UPF1 when cells were irradiated with 20 Gy (Figure S5). Kinetic analysis demonstrated maximal accumulation of UPF1 on chromatin 2 hr after irradiation. Interestingly, the DNA-repair factor Ku86 accumulated on chromatin with kinetics similar to UPF1, whereas γ-H2AX peaked after 1 hr (Figure 3B).

To investigate the role of different PIKKs in promoting association of UPF1 with chromatin, we transfected HeLa cells with shRNAs against ATM, ATR, and SMG1 kinases (see Figure S1). Four days after transfection, we γ-irradiated the cells with 10 Gy and prepared soluble and chromatin-bound protein fractions. ShRNA-mediated depletion of ATM did not affect the γ-irradiation-induced chromatin association of UPF1 (Figure 3C). On the contrary, depletion of SMG1 induced 3-fold-higher levels of soluble and chromatin-bound UPF1 protein in both untreated and γ-irradiated samples (Figure 3C). Given that SMG1-shRNA induces DNA damage ([9] and our unpublished results), we speculate that the higher amounts of chromatin-bound UPF1 may be a cellular response to DNA damage. When ATR was depleted, the levels of chromatin-bound UPF1 were reduced to 60% as compared to the empty-vector-treated cells, demonstrating a critical role of this kinase for loading UPF1 onto chromatin during normal cell-cycle progression. In addition, UPF1 did not accumulate on chromatin in response to γ irradiation in ATR-depleted cells (Figures 3C and 3D). Importantly, although the achieved degree of ATR depletion impaired the ability of UPF1 to associate with chromatin, it did not affect NMD as measured with the β-Globin^{NS39} reporter and ABCC4^{SV2} (Figure 3D). Because β-globin^{NS39} NMD has been reported to occur predominantly in nuclear-associated fractions of the cells [23], we also analyzed RNA prepared from nuclear fractions and obtained similar results (data not shown). Thus, the ATR-dependent association of UPF1 with chromatin has no apparent function in NMD.

Human UPF1 is a phosphoprotein containing 28 S/T-Q consensus sites for PIKKs, and at least one serine near the C terminus (S1096) is a known target of the SMG1 kinase during NMD [24]. To test whether chromatin association of UPF1 correlates with PIKK-mediated phosphorylation, endogenous UPF1 was immunoprecipitated from soluble and DNase fractions from HeLa cells and the relative proportion of phospho-UPF1 in each fraction was determined in western blots with anti-phospho-S/T-Q antibodies. The relative amount of phospho-UPF1 was 2.5-fold higher in chromatin bound versus unbound fraction (Figure 3E). Enrichment of phospho-UPF1 on chromatin was also seen when we overexpressed a Flag-tagged version of UPF1 and performed immunoprecipitation experiments with anti-Flag antibodies (data not shown). These results raise the possibility that the observed ATR-dependent chromatin loading of UPF1 is directly regulated by ATR-mediated phosphorylation. Therefore, we performed an in vitro kinase assay by incubating Flag-tagged UPF1 protein with ATR or ATR kinase-dead (ATR^{KD}) proteins in the presence of γ[^{32}P] ATP. Reactions were analyzed by SDS-PAGE and autoradiography. UPF1 was phosphorylated in the reaction containing active ATR, whereas barely any phospho-UPF1 was detected in the reaction samples containing ATR^{KD} (Figure 3F). The residual phosphorylation observed in the ATR^{KD} samples may be due to traces of endogenous active ATR, coimmunoprecipitated with Flag-tagged ATR^{KD} (Figure 3F). Consistently, we found that shRNA-mediated depletion of ATR substantially reduces the levels of phosphorylated UPF1 in the cell (Figure 3G). Thus, ATR is a UPF1 kinase in vitro and is required for UPF1 phosphorylation in vivo. It has been reported that γ irradiation induces SMG1- and ATM-dependent phosphorylation of UPF1 [9]. However, shRNA-mediated depletion of SMG1 and ATM did not interfere with the chromatin association of UPF1 (Figure 3C), even though SMG1 and ATM functions were partially lost (see Figure S1). We conclude that ATR-mediated phosphorylation regulates UPF1 loading onto chromatin during normal cell-cycle progression. Furthermore, γ irradiation triggers not only SMG1- and ATM-dependent phosphorylation of UPF1, but also ATR-dependent phosphorylation events that lead to UPF1 accumulation onto chromatin. The timing of UPF1 loading onto chromatin upon γ irradiation (Figure 3B, see above) is consistent with ATR regulating the late phase (2–9 hr after irradiation) of the response to IR [25].

What is the function of chromatin-bound UPF1? Human UPF1 may sustain genome stability as a component of DNA replication and/or repair machineries. In support of this hypothesis, it has been reported that bovine UPF1 copurifies with polymerase δ and ectopically expressed human UPF1 coimmunoprecipitated with the

separated by SDS-PAGE, transferred to nitrocellulose filters, and subjected to autoradiography. Protein amounts were controlled by probing the same filters with anti-UPF1 and anti-ATR antibodies. The lower band in the upper panel may represent an ATR substrate coimmunoprecipitating with ATR proteins.

(G) HeLa cells were transfected with shRNA against ATR and empty-vector controls. Five days after transfection, total proteins were prepared and immunoprecipitation and western-blot experiments were performed as in (E) Numbers indicate the mean ratio of anti-phospho-S/T-Q signal relative to the anti-UPF1 signal, after normalization to the empty-vector sample.

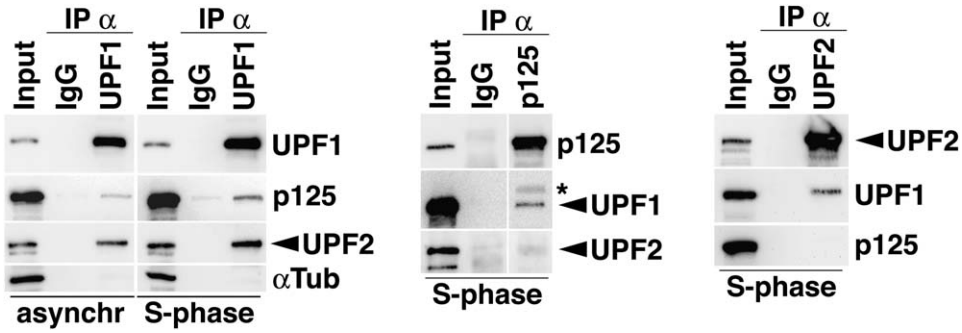

Figure 4. UPF1 Interacts with DNA Polymerase δ

HeLa cells were treated with 2 mM hydroxyurea for 24 hr and then released into S phase for 2 hr or left asynchronous. Total-cell extracts were prepared, and endogenous UPF1 (left), p125 catalytic subunit of pol δ (middle), and UPF2 (right) were immunoprecipitated with specific antibodies. Immunoprecipitates were resolved by SDS-PAGE and analyzed by western blotting with the antibodies indicated on the right. IgGs were used as control for immunoprecipitation specificity. The unrelated α-Tubulin is not detected in the UPF1 immunoprecipitates. The asterisk indicates a band of unknown nature reactive to UPF1 antibodies.

endogenous p66 subunit of pol δ in HeLa cell extracts [26]. To corroborate this interaction, we prepared total-protein extracts from HeLa cells that were unsynchronized or synchronized in S phase. Reciprocal coimmunoprecipitation of UPF1 and the catalytic subunit of pol δ (p125) was observed, and this interaction was enhanced in S phase (Figure 4). Physical association of UPF1 was also observed with the NMD factor UPF2, whereas no interaction was detected between UPF2 and p125 (Figure 4). Thus, UPF1 seems to assemble into distinguishable complexes to perform functions in NMD (with UPF2) and DNA synthesis (with pol δ). It is conceivable that UPF1 DNA helicase activity assists pol δ to facilitate fork progression or DNA repair. In addition, UPF1 may participate in S phase progression and DNA repair through regulation of specific mRNAs. Kaygun and Marzluff have recently demonstrated that both UPF1 and ATR are required for the regulated degradation of replication-dependent histone mRNAs when cells exit S phase and after hydroxyurea treatment [27]. It is possible that in response to DNA damage and during replication, ATR-mediated phosphorylation and chromatin loading of UPF1 are important for the degradation of these mRNAs.

In conclusion, our results demonstrate for the first time that UPF1 is essential for human cells to progress through S phase, protecting against genome instability. We suspect that the cell lethality induced by UPF1 depletion as well as the embryonic death observed in UPF1-KO mice [28] may derive (at least in part) from a failure in DNA replication. The fact that yeast and worm UPF1 mutants are viable, even though the degradation of PTC-containing mRNAs is extinguished [29–31], could indicate that the essential role for UPF1 in DNA replication and genome stability is an evolutionarily late acquisition. However, further studies that assess DNA replication in yeast and worm UPF1 mutants are required to elucidate this point.

Our study, together with other recently published data [9–11, 27], points to unexpected new roles for NMD factors in DNA replication, DNA repair, and telomere integrity. Thus, these components seem to sit at the crossroads between DNA and RNA surveillance networks, and they may function in a complex to coordinate the global cellular response to replicative and genotoxic stresses. It will be fascinating to discover whether these multiple roles are genetically separable.

Supplemental Data

Supplemental Data include Supplemental Experimental Procedures and five figures and are available with this article online at: http://www.current-biology.com/cgi/content/full/16/4/433/DC1/.

Acknowledgments

We thank P. Reichenbach for vector construction, M. Migliaccio for help in FACS analysis, T.R. Brummelkamp for the pSUPER vector, M.W. Hentze for human UPF1 cDNA, O. Muehlemann for HeLa β-globin reporter cells, P. Nghiem for GK41 and GW33 cells, S. Ohno for the SMG1 antibody, and J.Wittmann and H.-M. Jäck for the UPF2 shRNA vectors and the UPF2 antibody. We thank M. Cockell, J.P. Cooper, and V. Simanis for critical reading of the manuscript and the members of our laboratory for helpful discussions. We are supported by grants from the Swiss National Science Foundation, the Swiss Cancer League, and the FP6-programme of the European Union.

Received: September 14, 2005
Revised: December 12, 2005
Accepted: January 10, 2006
Published: February 21, 2006

References

1. Holbrook, J.A., Neu-Yilik, G., Hentze, M.W., and Kulozik, A.E. (2004). Nonsense-mediated decay approaches the clinic. Nat. Genet. *36*, 801–808.
2. Mendell, J.T., Sharifi, N.A., Meyers, J.L., Martinez-Murillo, F., and Dietz, H.C. (2004). Nonsense surveillance regulates expression of diverse classes of mammalian transcripts and mutes genomic noise. Nat. Genet. *36*, 1073–1078.
3. Hentze, M.W., and Kulozik, A.E. (1999). A perfect message: RNA surveillance and nonsense-mediated decay. Cell *96*, 307–310.
4. Mango, S.E. (2001). Stop making nonsense: The C. elegans smg genes. Trends Genet. *17*, 646–653.
5. Iborra, F.J., Escargueil, A.E., Kwek, K.Y., Akoulitchev, A., and Cook, P.R. (2004). Molecular cross-talk between the transcription, translation, and nonsense-mediated decay machineries. J. Cell Sci. *117*, 899–906.
6. Maquat, L.E. (2004). Nonsense-mediated mRNA decay: Splicing, translation and mRNP dynamics. Nat. Rev. Mol. Cell Biol. *5*, 89–99.
7. Wilkinson, M.F. (2005). A new function for nonsense-mediated mRNA-decay factors. Trends Genet. *21*, 143–148.

8. Kim, Y.K., Furic, L., DesGroseillers, L., and Maquat, L.E. (2005). Mammalian Staufen1 recruits Upf1 to specific mRNA 3′UTRs so as to elicit mRNA decay. Cell *120*, 195–208.
9. Brumbaugh, K.M., Otterness, D.M., Geisen, C., Oliveira, V., Brognard, J., Li, X., Lejeune, F., Tibbetts, R.S., Maquat, L.E., and Abraham, R.T. (2004). The mRNA surveillance protein hSMG-1 functions in genotoxic stress response pathways in mammalian cells. Mol. Cell *14*, 585–598.
10. Reichenbach, P., Hoss, M., Azzalin, C.M., Nabholz, M., Bucher, P., and Lingner, J. (2003). A human homolog of yeast Est1 associates with telomerase and uncaps chromosome ends when overexpressed. Curr. Biol. *13*, 568–574.
11. Snow, B.E., Erdmann, N., Cruickshank, J., Goldman, H., Gill, R.M., Robinson, M.O., and Harrington, L. (2003). Functional conservation of the telomerase protein Est1p in humans. Curr. Biol. *13*, 698–704.
12. Lamba, J.K., Adachi, M., Sun, D., Tammur, J., Schuetz, E.G., Allikmets, R., and Schuetz, J.D. (2003). Nonsense mediated decay downregulates conserved alternatively spliced ABCC4 transcripts bearing nonsense codons. Hum. Mol. Genet. *12*, 99–109.
13. Wittmann, J., Hol, E.M., and Jack, H.-M. (2005). HUPF2 silencing identifies physiologic substrates of mammalian nonsense-mediated mRNA decay. Mol. Cell. Biol., *26*, 1272–1287.
14. Madsen, P., and Celis, J.E. (1985). S-phase patterns of cyclin (PCNA) antigen staining resemble topographical patterns of DNA synthesis. A role for cyclin in DNA replication? FEBS Lett. *193*, 5–11.
15. Bravo, R., and Macdonald-Bravo, H. (1987). Existence of two populations of cyclin/proliferating cell nuclear antigen during the cell cycle: Association with DNA replication sites. J. Cell Biol. *105*, 1549–1554.
16. Ward, I.M., and Chen, J. (2001). Histone H2AX is phosphorylated in an ATR-dependent manner in response to replicational stress. J. Biol. Chem. *276*, 47759–47762.
17. Bakkenist, C.J., and Kastan, M.B. (2004). Initiating cellular stress responses. Cell *118*, 9–17.
18. Sancar, A., Lindsey-Boltz, L.A., Unsal-Kaccmaz, K., and Linn, S. (2004). Molecular mechanisms of mammalian DNA repair and the DNA damage checkpoints. Annu. Rev. Biochem. *73*, 39–85.
19. Nghiem, P., Park, P.K., Kim Ys, Y.S., Desai, B.N., and Schreiber, S.L. (2002). ATR is not required for p53 activation but synergizes with p53 in the replication checkpoint. J. Biol. Chem. *277*, 4428–4434.
20. Krause, D.R., Jonnalagadda, J.C., Gatei, M.H., Sillje, H.H., Zhou, B.B., Nigg, E.A., and Khanna, K. (2003). Suppression of Tousled-like kinase activity after DNA damage or replication block requires ATM, NBS1 and Chk1. Oncogene *22*, 5927–5937.
21. Zhou, N., Xiao, H., Li, T.K., Nur, E.K.A., and Liu, L.F. (2003). DNA damage-mediated apoptosis induced by selenium compounds. J. Biol. Chem. *278*, 29532–29537.
22. Riva, F., Savio, M., Cazzalini, O., Stivala, L.A., Scovassi, I.A., Ducommum, B., and Prosperi, E. (2004). Distinct pools of proliferating cell nuclear antigen associated to DNA replication sites interact with the p125 subunit of DNA polymerase delta or DNA ligase I. Exp. Cell Res. *293*, 357–367.
23. Thermann, R., Neu-Yilik, G., Deters, A., Frede, U., Wehr, K., Hagemeier, C., Hentze, M.W., and Kulozik, A.E. (1998). Binary specification of nonsense codons by splicing and cytoplasmic translation. EMBO J. *17*, 3484–3494.
24. Ohnishi, T., Yamashita, A., Kashima, I., Schell, T., Anders, K.R., Grimson, A., Hachiya, T., Hentze, M.W., Anderson, P., and Ohno, S. (2003). Phosphorylation of hUPF1 induces formation of mRNA surveillance complexes containing hSMG-5 and hSMG-7. Mol. Cell *12*, 1187–1200.
25. Brown, E.J., and Baltimore, D. (2002). Essential and dispensable roles of ATR in cell cycle arrest and genome maintenance. Genes Dev. *17*, 615–628.
26. Carastro, L.M., Tan, C.K., Selg, M., Jack, H.M., So, A.G., and Downey, K.M. (2002). Identification of delta helicase as the bovine homolog of HUPF1: Demonstration of an interaction with the third subunit of DNA polymerase delta. Nucleic Acids Res. *30*, 2232–2243.
27. Kaygun, H., and Marzluff, W.F. (2005). Regulated degradation of replication-dependent histone mRNAs requires both ATR and Upf1. Nat. Struct. Mol. Biol. *12*, 794–800.
28. Medghalchi, S.M., Frischmeyer, P.A., Mendell, J.T., Kelly, A.G., Lawler, A.M., and Dietz, H.C. (2001). Rent1, a trans-effector of nonsense-mediated mRNA decay, is essential for mammalian embryonic viability. Hum. Mol. Genet. *10*, 99–105.
29. Czaplinski, K., Weng, Y., Hagan, K.W., and Peltz, S.W. (1995). Purification and characterization of the Upf1 protein: A factor involved in translation and mRNA degradation. RNA *1*, 610–623.
30. Leeds, P., Peltz, S.W., Jacobson, A., and Culbertson, M.R. (1991). The product of the yeast UPF1 gene is required for rapid turnover of mRNAs containing a premature translational termination codon. Genes Dev. *5*, 2303–2314.
31. Page, M.F., Carr, B., Anders, K.R., Grimson, A., and Anderson, P. (1999). SMG-2 is a phosphorylated protein required for mRNA surveillance in Caenorhabditis elegans and related to Upf1p of yeast. Mol. Cell. Biol. *19*, 5943–5951.